Friedrich-Alexander-Universität
Naturwissenschaftliche Fakultät

Bachelor Thesis

in Physics

Position calibration with the acoustic receivers of Km3NeT

Valentin Schwieger

Supervisor: apl. Prof. Dr. Robert Lahmann

Erlangen Centre for Astroparticle Physics

Submission date: 14.07.2025

Abstract

This thesis presents a method for reconstructing positions in the KM3NeT-ORCA detector using the arrival times of acoustic signals from a moving source. First, a plane wave approximation is used to estimate the signal direction, followed by a full multilateration fit based on spherical wavefronts and realistic sound speed profiles. It is shown that the sound speed model has a clear impact on the reconstruction accuracy. The final results achieve position uncertainties on the order of one meter and show systematic offsets of a few meters, depending on model assumptions. In a second step, the method is inverted to determine detector unit (DU) positions based on known source positions, reaching sub-meter precision. The results confirm that acoustic positioning in KM3NeT works reliably when the geometry is favorable and the data quality is high.

Contents

1 Introduction

Neutrino detection is a difficult task for scientists all over the world. These particles hardly ever interact with anything. This property, however, makes them an interesting source of information about the cosmos. Neutrinos can travel huge distances through space without being absorbed or deflected, even when passing through stars or entire galaxies. That means they carry direct information from the places where they were created like the core of the sun, exploding stars (supernovae) or even more extreme objects like black holes. Since they interact so weakly, they reach earth unchanged and can give insight into processes and regions of the universe that are otherwise invisible. But since they interact so weakly, it's nearly impossible to see them with a small detector. That's why the neutrino detectors need to get bigger and bigger to maximize the probability of a neutrino interaction [1]. The core of KM3NeT („Cubic-kilometer (km^3) Neutrino Telescope“) is an observatory located in the Mediterranean Sea consisting of two main telescopes: ARCA (Astroparticle Research with Cosmics in the Abyss) and ORCA (Oscillation Research with Cosmics in the Abyss). Their positions can be seen in figure 1. These telescopes use seawater as the detector material and can observe massive volumes of water in search of neutrino interactions in the form of Cherenkov radiation, which can be detected using photomultipliers.

Figure 1: Position of the two main detectors of Km3NeT in the Mediterranean sea [2].

The Cherenkov radiation is emitted when a charged particle travels faster than the local speed of light in a medium like water in this case. This radiation is faint and directional, allowing the reconstruction of particle trajectories and energies. Since

KM3NeT aims to measure these signals with high precision, the exact positions of the photomultipliers must be known at all times. This positioning happens via acoustic signals and trilateration under water. The digital optical modules (DOMs), which house the photomultipliers, are mounted on flexible lines that move with the sea current, so their positions are constantly changing. To track these changes, two separate acoustic systems are installed to ensure the positioning with the required accuracy [3].

On July 9th 2024 a research ship passed by the ORCA telescope, which is located offshore the coast of Toulon in France. The ship sent acoustic signals that the hydrophones of the positioning system recorded [4]. In this Bachelor thesis I will study some of the recorded data and try to reconstruct the position of the ship by comparing the time of arrival of the same signal at different hydrophones. This process will help with understanding the accuracy of the positioning system and will give new insight into the positioning process [5]. Moreover, by comparing reconstructed positions to known ship tracks, the performance of the acoustic triangulation method can be independently tested, which is especially valuable for verifying the calibration of the detector's infrastructure.

The first chapter introduces the KM3NeT experiment and focuses on the structure of the ORCA detector, since the data used in this thesis originates from it. The reconstruction of the ship's position is carried out using a fitting method, and for this purpose, the program `Iminuit` is used. Therefore, the second chapter will explain how `Iminuit` works and how it can be applied. The third chapter is dedicated to the sea mission conducted above ORCA, followed by a section on the necessary steps for data processing and analysis. Finally, the results of the three different fits performed in the course of this thesis will be presented and discussed.

2 Km3NeT

The KM3NeT collaboration is a project of scientists, engineers, and institutions from more than ten European countries, including France, Italy, the Netherlands, Greece, and Germany. KM3NeT is the organizer of the projects which are also supported by research organizations such as CNRS in France, INFN in Italy, NWO in the Netherlands, and many universities and laboratories throughout Europe. KM3NeT is funded by national science foundations, the European Union, and public research funding bodies [5]. The ARCA Telescope is capable of detecting neutrinos generated by the most powerful and farthest astrophysical sources like active galactic nuclei, supernovae, gamma-ray-bursts, and colliding neutron stars. Neutrinos have the property of traveling the universe without much disturbance, so they carry the most intact information from their sources in contrast to photons or charged parti-

cles which are scattered or absorbed on their way to Earth. This makes it a strong instrument for astronomy [5]. Other than the astrophysics field, the KM3NeT research is also of importance for fundamental particle physics, particularly due to its ORCA (Oscillation Research with Cosmics in the Abyss) section. The ORCA project is aiming at investigating the neutrino oscillations, which is a quantum effect of neutrinos switching their type almost randomly. ORCA's objective is to find out which neutrino mass is preferred and why by accurately detecting oscillations. The neutrino mass hierarchy is still unexplained. Explaining this would be a big step forward for the Standard Model and beyond [5]. In addition to the physics objectives of KM3NeT, it is also engaged in technological innovation, marine science, and international partnership. The infrastructure that has been set up in the oceans is a great source of information about marine life, oceanography, and geophysics, thus KM3NeT is a multifunctional observatory [5].

2.1 Detector setup at ORCA

The Oscillation Research with Cosmics in the Abyss (ORCA) detector is one of the two main components of the KM3NeT infrastructure, located in the Mediterranean Sea near Toulon, France. ORCA is specifically optimized for the detection of atmospheric neutrinos with energies in the range of a few GeV, which are crucial for studying neutrino mass hierarchy and oscillation parameters [3]. The ORCA Telescope consists of 23 separate Detection Units, also known as DU's. Every DU consists of 18 different vertically spaced Digital Optical Modules (DOM), each containing 31 photomultipliers. The DUs are anchored to the see floor and fixed on top with a buy as can be seen in figure 2. Due to currents or other turbulations in the water, the position of each DOM is variable. That's why hydrophones are installed, that can guarantee precise positioning under water.

Due to strong absorption of electromagnetic radiation in seawater, the method of using radio or optical signals for long-range communication or positioning is practically impossible. The ocean severely limits the use of radio or optical signals for long-range communication or positioning because of the rapid attenuation of electromagnetic radiation in seawater. Acoustic waves have an advantage over optical and radio waves since they suffer from much less attenuation and can propagate over several kilometers in the ocean depths. This inherent characteristic makes sound waves the only feasible choice for underwater positioning systems [6, 7]. At the KM3NeT neutrino telescope, the positioning of the detection elements is something that has to be continuously and accurately done with high precision, because of the flexibility of the Detection Units and sea currents that can displace them. During the deployment process, the absolute position of the lower end of each DU, which is fixed to

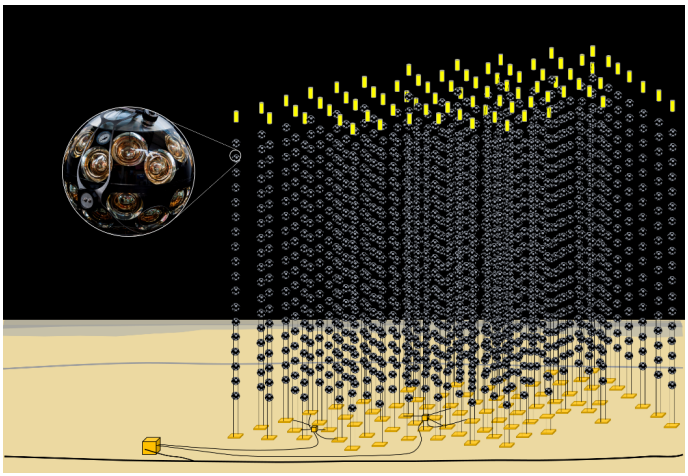

Figure 2: An artist impression of the layout of an Km3NeT detector the DU's are anchored to the seafloor and stabilized by a yellow buy. One DOM is shown in detail. The round spots are the photo multipliers [5].

the seabed, is determined using the Navigation and Absolute Acoustic Positioning System (NAAPS) [8]. This source of locational information acts as a fixed baseline for all other registration measurements. KM3NeT relies on the Relative Acoustic Positioning System (RAPS) for the real-time tracking of the Digital Optical Modules (DOMs) along the DUs. To accomplish this, there are acoustic emitters and receivers installed that are built right into the infrastructure. The acoustic emitters of the NAAPS are called acoustic beacons and they are spaced outside of the DU formation. When using triangulation, the distances between various parts of the detector can be calculated from the travel times of the acoustic signals between the different known positions of the emitters and receivers [3].

2.2 ORCA Footprint

The ORCA array currently consists of 23 DUs arranged in a dense oblique Bravis lattice, the formation visible in figure 3. The layout of the ORCA detector is optimized for the detection of low-energy atmospheric neutrinos, typically in the range of a few GeV. Because these neutrinos produce relatively short particle tracks in water, a high granularity of the optical modules is necessary to ensure accurate reconstruction of the interaction topology and kinematics [3, 9].

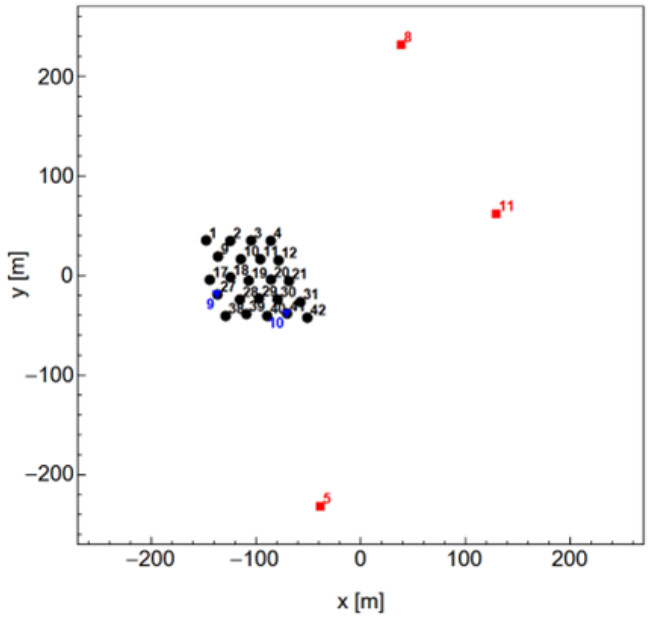

Figure 3: A layout of the ORCA footprint on the seafloor. The DU's (black) are spaced in a lattice. The red squares are the acoustic beacons that can emit acoustic signals for triangulation.

To meet this requirement, the Detection Units (DUs) in ORCA are deployed much closer together than in ARCA. The vertical spacing between the Digital Optical Modules (DOMs) in ORCA is about 9 meters, and the horizontal spacing between DUs is approximately 20 meters. In contrast, ARCA, which is designed to detect high-energy neutrinos above several TeV, uses a much larger spacing of approximately 36 meters between DOMs and over 90 meters between DUs [9, 8].

2.3 Hydrophones in KM3NeT-ORCA

Each DOM of the KM3NeT-ORCA detector is equipped with a piezoelectric acoustic sensor. This sensor is fixed on the inside of the glass sphere. These sensible sensors serve as hydrophones and have multiple purposes, including acoustic positioning, ambient noise monitoring, and detection of calibration signals. The piezo elements are sensitive to acoustic frequencies in the range of 2–125 kHz. They are directly coupled to a preamplifier and a digitizing system within the DOM [10].

The hydrophones digitize the acoustic signals at a sampling rate of 195.3 kHz. The gathered data is sent to shore via the optical network of the detector and further processed by the onshore Data Acquisition System (DAQ). This process allows more precise data analysis for Time-of-Arrival (ToA) measurements and faster positioning corrections [10, 11].

3 Speed of sound in sea water

A sound wave is generated by a change of pressure in respect to the equilibrium. The speed of propagation in an acoustic medium is described by

$$c^2 = \frac{\partial P}{\partial \rho} \tag{1}$$

That means that the speed of sound c is a measure of how the density of the acoustic medium changes with a variation in pressure. If small changes in density result in large changes in pressure, the speed of sound is fast [12].
In the seawater, the speed of sound is mostly dependent on three parameters: the temperature, the salinity, and the pressure.
Temperature has the greatest impact on how fast sound travels in seawater, especially near the surface. When the water gets warmer, the molecules move around more because they have more energy. This leads to more collisions between them, which helps sound waves move through the water more quickly. So, in warmer water, the speed of sound increases. This effect is strongest close to the surface where the temperature changes a lot with depth. In deeper waters, the temperature changes only slightly and mostly stays constant [13]. In the Mediterranean Sea, this effect is very drastically seen. Figure 4 shows the behavior of the temperature near the location of the ORCA detector.

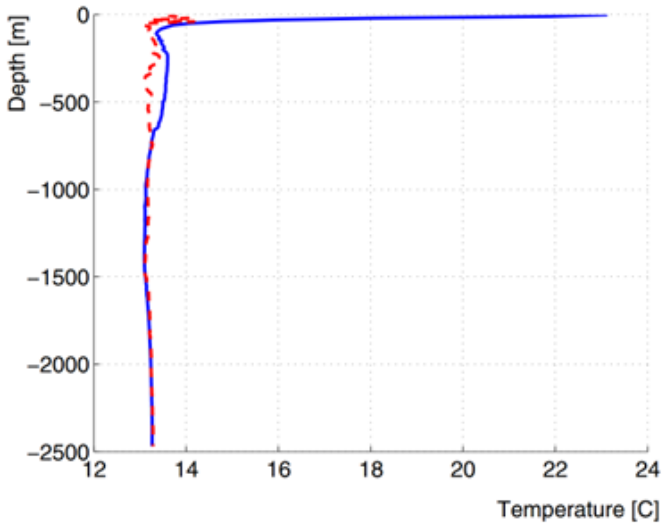

Figure 4: Variation of the temperature with depth. It changes rapidly near the surface and then reaches a constant level. The blue line is a measurement in August after the summer months and the red one is a measurement in spring. These measurements were conducted in the Mediterranean Sea near the ORCA site.

Salinity affects the density and compressibility of seawater. An increase in salinity increases the speed of sound, though the effect is more modest compared to

temperature. As depth increases, so does pressure. Higher pressure compresses the water slightly, so under pressure it becomes denser and harder to compress, and thus the speed of sound gains. The speed of sound increases by about 1.7 m/s per 100 m of depth, making pressure the dominant factor at great depths, because temperature reaches a lower limit fast.
These three factors interact in complex ways. Near the surface, temperature dominates, often resulting in a sound speed maximum at shallow depths. But the effect of the temperature can be neglected going deeper because it reaches a constant value. Due to the linear growth of the pressure with depth, the speed of sound grows linearly with depth at constant temperature [13].

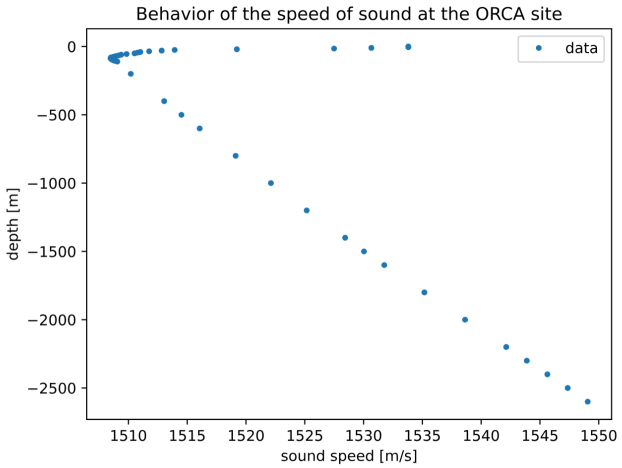

Figure 5: That behavior can be seen in this plot which contains data from a measurement of the sound speed dependent on the depth conducted directly at the ORCA site.[1]

It can be seen in figure 5 that in the Mediterranean Sea the speed of sound changes very drastically at the surface. Hence, a selection of a correct model which represents the speed of sound is crucial for getting an accurate fit since the time of travel of the signal is directly related to the way the sound travels in the medium. In case the sound speed profile is not consistent with the actual situation, the position reconstruction can be off to a large extent. Therefore, using authentic and local sound speed information makes the fit more reliable.

[1]Data obtained from Sharif El Mentawi/Vincent Bertin (CPPM), May 2025.

4 The `Iminuit` library

`Iminuit` is a Python library designed for numerical minimization, which is particularly well-suited for problems in scientific data analysis. It provides a Python interface to the MINUIT2 minimizer, a software originally developed at CERN (the European Organization for Nuclear Research) [14].

4.1 Functionality and outputs of `Iminuit`

The fit procedure starts by defining a function that encodes how well a choice of parameters matches the data. This function is often a chi-squared function, denoted χ^2. The lower this function's value, the better the model fits the data. `Iminuit` finds the parameter values that minimize this function.

$$\chi^2 = \sum_{i=1}^{n} \left(\frac{y_i - f(x_i; \theta)}{\sigma_i} \right)^2 \tag{2}$$

To find the minimum of this function, `Iminuit` follows an algorithm called MIGRAD. This algorithm gets an initial guess for the parameters θ and checks how the function changes when each parameter changes. From the evaluations, it estimates the gradient of the function. It changes the parameters values in the direction of the most rapid decrease. This process is repeated iteratively and the algorithm lowers the step size each iteration as it approaches the minimum [14].
`Iminuit` allows to set parameter limits. In a physical system this is often important because there are solutions that don't represent the real world. By setting the limits to a physically plausible interval it is ensured that the resulting solution is correct. The limits, however, do affect the minimization procedure. It transforms the internal variable P_{int} into an external variable P_{ext} which ranges from lower bound to upper bound via a trigonometry function.

$$P_{ext} = a + \frac{b-a}{2} (\sin P_{int} + 1) \tag{3}$$

The internal variable can take on any value, while the external variable can take on values only between the lower limit a and the upper limit b. So the result is an approximation of a linear problem and this has side effects. Near the boundaries where $\partial P_{ext}/\partial P_{int} \approx 0$ the program cannot give a meaningful result for the parameter and its errors [14].
`Iminuit` also receives information about how the χ^2 function curves around the minimum. This is important because the curvature around the minimum indicates how sensitive the function is to changes in each parameter. Strong curvature means that the parameter is well constrained and has small uncertainty, while minimal cur-

vature means that the parameter is not well determined. This curvature is encoded in the Hessian matrix. Once the minimum is found, `Iminuit` returns the best-fit parameter values and their errors that are computed from the Hessian matrix. Parameter correlations are also returned, which indicate how changes in one parameter affect others. If parameters are very strongly correlated, then one of the parameters can be discarded or the choice of parameters should be renewed completely [15].
The minimization stops when the changes in the function value and in the parameters become smaller than a certain threshold and the estimated distance to the minimum (EDM) is below a predefined limit. These criteria ensure that a local minimum has been reached with reasonable precision. The minimization also stops automatically if the number of function evaluations exceeds a predefined maximum (by default, 10000). This ensures that the algorithm does not run indefinitely in case the function has no well-defined minimum or if the convergence is too slow. If this happens, the fit usually terminates with a warning and the status flag will indicate that the result is not reliable. In such cases, improving the initial parameter guesses, checking the χ^2 function, or relaxing parameter limits can help. The stopping conditions can be tuned but usually the default values are sufficient.

Once the fit is complete, `Iminuit` prints several useful outputs. The best-fit parameter values and their uncertainties are displayed, along with the χ^2 value at the minimum and the number of degrees of freedom. The uncertainties are estimated using the inverse of the Hessian matrix. Figure 6 shows how the best fit parameters are displayed along with their errors.

	Name	Value	Hesse Error	Minos Error-	Minos Error+	Limit-	Limit+	Fixed
0	a	0.002	0.029					
1	b	0.500	0.005					
2	sigma	0.98	0.04			0		

Figure 6: This is the table of the best fit parameter values and their corresponding hessian errors. It can be seen that a lower limit has been applied to the parameter `sigma` which ensures that it stays greater than 0 [15].

The correlation matrix, as displayed in figure 7, shows how strongly the fit parameters are correlated. Values close to ± 1 indicate strong correlations, meaning that changing one parameter would significantly affect the others.

	a	b	sigma
a	0.000839	0.004e-3 **(0.030)**	-0 **(-0.027)**
b	0.004e-3 **(0.030)**	2.43e-05	-0.141e-3 **(-0.718)**
sigma	-0 **(-0.027)**	-0.141e-3 **(-0.718)**	0.0016

Figure 7: This is the displayed correlation matrix which is color coded. The darker the color, the higher the covariance until it reaches a dark red approaching ± 1 [15].

Other diagnostics such as the status flags, the EDM (estimated distance to minimum), and the number of function calls are also printed. A low EDM and a status flag of 0 usually mean that the fit converged successfully. If the status flag is nonzero or the EDM is too high, the result should be treated with caution. The outputs of the `Migrad` algorithm can be displayed like in figure 8 to check the validity of the results.

Migrad	
FCN = -8.774e+04	Nfcn = 95
EDM = 1.33e-06 (Goal: 0.0002)	time = 12.5 sec
Valid Minimum	Below EDM threshold (goal x 10)
No parameters at limit	Below call limit
Hesse ok	Covariance accurate

Figure 8: This is the most important output of `iminuit`. It displays the final value of the χ^2 function (FCN), the estimated distance to the minimum (EDM), the number of tries and the time it took (Nfcn). Additionally, there is a color coded field that basically tells if the fit is valid. If any of the stats is at yellow or worse at purple, the fit results are not fully reliable [15].

4.2 The χ^2 distribution

The χ^2 distribution is a common distribution in statistics. It naturally arises in problems in situations like fitting. It can be formed by summing up the square of independent normally distributed random variables Z_i. The statistical distribution of a variable

$$\chi^2 = \sum_{i=1}^{n} Z_i^2 \tag{4}$$

is a χ^2_n distribution with n degrees of freedom. For large values of n the χ^2 distribution converts to a normal distribution. The behavior of the probability density of the χ^2 distribution for different degrees of freedom is visualized in figure 9 to get a better intuition[16].

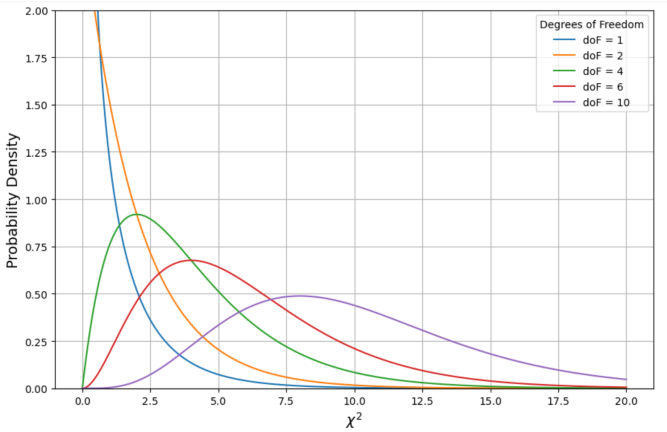

Figure 9: The behavior of the probability density of the χ^2 distribution for different degrees of freedom (doF). For large numbers of doF this resembles a normally distributed variable.

The concept works under the assumption that the random variables Z_i are normally distributed with an expectation of 0 and a variance of 1. With this the expectation of Z_i^2 can be derived. (Notation: $E[x]$ is the expectation of x, also $E[ax + y] = aE[x] + E[y]$ is linear, which stems from the linearity of the integral)

$$Var(Z) := E[(Z - E[Z])^2] = E[Z^2] - 2ZE[Z] + E[Z]^2 \tag{5}$$

Note that $E[Z] = 0$ and take the expectation of both sides (expectation of a constant value is the value itself) which leads to the result.

$$Var(Z) = E[Z^2] - 0 + 0^2 = E[Z^2] = 1 \tag{6}$$

This result holds because the assumption was a variance of 1. Now it can be concluded that for independent random variables, the expectation of the sum is just $\sum_n 1 = n$. The behavior of the χ^2 distribution can be studied for different degrees of freedom.

4.3 Applications of the χ^2 distribution for the fit

Taking a look at the χ^2 function it is similar to a χ^2 distributed variable because it contains measurement which are always normally distributed and a model which describes the measured variable, so if the model is correct, the expectation of a single residuum would be 0. By dividing every residuum by the error of the measurement σ_i it is ensured, that the resulting variable has a variance of one. So with a perfect model the χ^2 function is χ^2 distributed. Without a fit, just by modeling the situation, the function of n measurements would be χ^2 distributed with n degrees of freedom. In the fit, variables are left open to be chosen freely by the fit program so that

the difference between the model and the data is minimized. As a result, after this process the residuals are not as independent as before. For every fit parameter chosen, the χ^2 distribution of the χ^2 function loses one degree of freedom. So, the distribution of the χ^2 function is a χ^2_{dof} distribution.

$$dof = \text{number of measurements} - \text{number of fit parameters} \tag{7}$$

Assumed that all the errors for the measured quantity are correct, the final value of the χ^2 function is a measure of the goodness of the model used. Statistically, it is expected that the mean value of the final χ^2 function for every measurement is equal to the degrees of freedom. If this value differs a lot, then the model used is imprecise or the fit went wrong. This method is called the χ^2 test. Another application is to scale the σ_i so that the function value equals the number of degrees of freedom. This method is used when the errors of the measurement are unknown, and the errors of the fit are of interest. By doing this it is implied that the model used is correct and the focus is on still getting valid errors for the fit parameters [17].

5 Sea campaign

On July 9th, 2024, a see campaign took place in the seas over the ORCA detector. The mission was to send signals from a small research ship and receive the signals with the hydrophones of the DU's. The event started in the morning at about 9 o'clock and ended in the afternoon on the same day. In this time, the ship followed a specific track above the detector as displayed in figure 10. The goal of the mission was to test an alternative triangulation of the ORCA DU anchors. For this a maximum number of hydrophone data is needed. For this thesis, the recovered time of arrival data of nine different DU's got analyzed and was, among other things, used to reconstruct the positions of the detection units using multilateration [4].

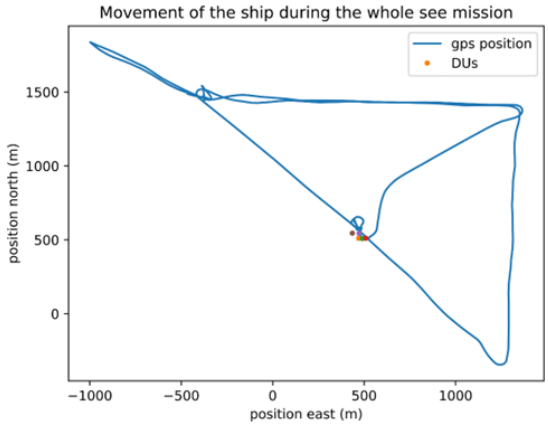

Figure 10: The gps position of the reserarch ship during the mission.

The data is split up into different runs which can be analyzed separately. Some runs are positioned directly over the detector, and some are further away. In this thesis, the data of two separate runs are analyzed. The first run (D0ORCA023_run_20711) was a circular motion directly over the DUs and the and the second run (D0ORCA023_run_20710)[2] was a triangular motion further away [4].

6 Data analysis

Before beginning with the fit, the data gathered from the different detection units must be filtered because it contains a lot of noise. The noise stems from the process of data acquisition. The system assigns a value to every cross-correlation it performs and saves this value along with the time of arrival. If this value called "quality factor" is high, then the hydrophone data was very similar to the waveform and if it is very low, the recorded signal was different to the compared waveform. This means that the quality factor of background noise can get very high by chance or the real signal can get canceled out by some other noise that interferes with it. When analyzing the data, the periodicity of the signal sent by the boat helps a lot, finding the right values in the noise. But sometimes it is not possible to determine the right time of arrival from the data and it is better to discard the value because the fit is of course very sensitive to small errors in time. The speed of sound at the sea floor is roughly 1,546 m/ms and the distance between the DUs is about 20 meters, so a change of milliseconds in the time of arrival can completely ruin the fit. A final test of the acquired data is to plot the time of arrival against the distance to the real position of the ship. A linear relationship is expected because the farther the distance, the longer the travel time. For the first run, the test reveals that there was an error with the data processing of two different DU's as displayed in figure 11.

They obviously do not match the linear progression. There is an offset of about two milliseconds to the value expected. A plausible explanation is, that the cross-corelation failed in determining the maximum of the waveform and assigned the wrong time of arrival. The exact reason for this is not clear. It is sure that the correlation still found the right signal because the waveform is about five milliseconds long, so the two millisecond offset is still in this range. Figure 12 shows the test applied to the data of the second run, the triangular motion.

[2]Data obtained from Sharif El Mentawi/Vincent Bertin (CPPM) May 2025

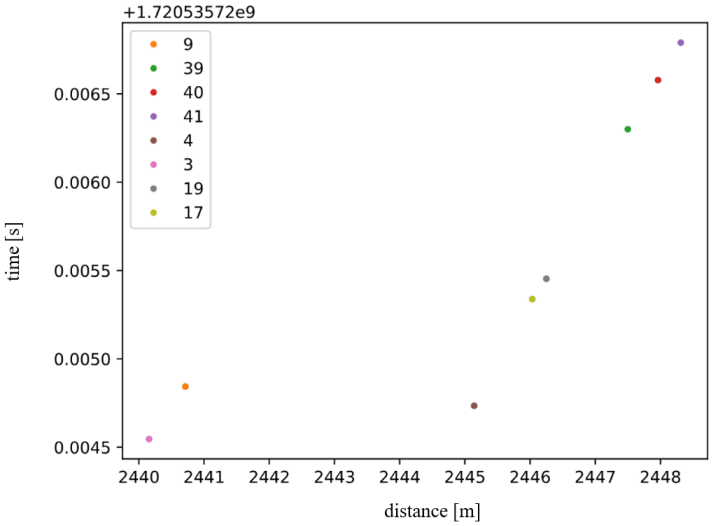

Figure 11: The time of arrival over the distance from DU to the ship which was calculated by using the real GPS positions. DU 9 and 3 have a constant offset in the data. The origin of the offset is not clear.

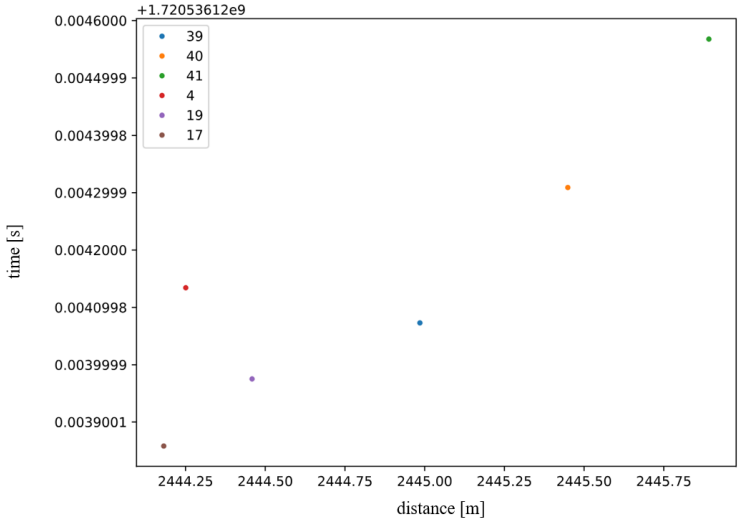

Figure 12: Additionally to 9 and 3, DU 4 is also faulty but with a smaller offset of only 0.2 milliseconds. Though very small this error is disturbing the fit greatly.

With these techniques the useful data is filtered. With the found time of arrivals the fit can finally be performed. The detection units that did not match the linear progression in the test will most probably not be part of the fits.

7 Fit of direction

The first goal is to reconstruct the correct direction of the ship with the time of arrivals at the different DU's. For this we assume a sound wave passing through the

water as a plane. The time of arrivals encode this plane: If a time is bigger than the others, then it means that the ship is far away from this DU. This is interpreted as a high point, while a low point is defined by a low time of arrival. The first step for this plane wave fit is to define a point where the plane hits the detectors. It is plausible to take the center point of all detection units. The plane can be described with this point and a vector, which is normal to it, the unit vector. The goal of the fit will be to find this unit vector to fully describe the plane wave of the sound signal passing through the detector. This also allows for an approximate reconstruction of the ship's position by following the vector of direction to the surface as displayed in figure 13.

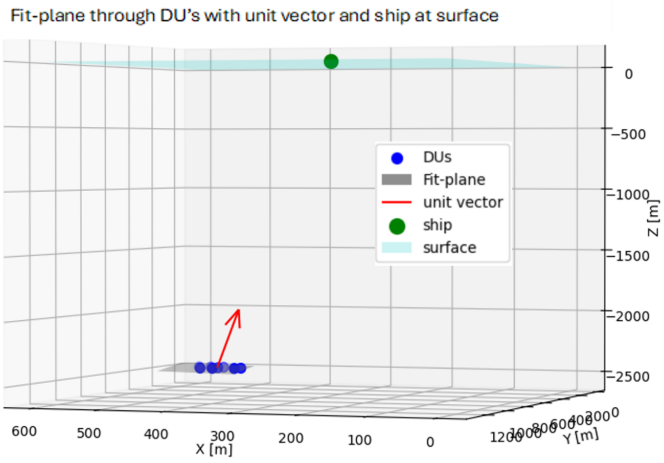

Figure 13: A sketch of how the plane wave fit works. It assumes a plane going through the detectors which is defined by the time of arrivals. The vector pointing at the position of the ship is the unit vector normal to the plane.

7.1 Model

For simplicity reasons the speed of sound in this fit is assumed as constant. This is not of interest because the goal of the fit is not to determine the position of the ship most accurately, but to test the data and get a first idea of the direction and the position of the ship, which can be useful later. The sound wave travels as a unit to the detector until it hits the first DU. From this point on it matters how fast the signal travels to the next DU's because this difference is what defines the plane. That's why the speed of sound on the sea floor is used. It's value is $c = 1546\,\mathrm{m/s}$.

A vector describes the plane. The length of the vector is irrelevant, so it can be assumed as one. This makes the fit much easier because only two parameters are needed to describe this unit vector. In spherical coordinates, these would be the

polar and azimuth angles θ and ϕ. The vector is described by

$$\vec{n}(\theta, \phi) = \begin{pmatrix} \sin\theta\cos\phi \\ \sin\theta\sin\phi \\ \cos\theta \end{pmatrix} \tag{8}$$

If $\vec{x_i}$ is the position of the i-th DU then the distance along the direction of propagation of the wave is the projection

$$d_i = (\vec{x_i} - \vec{x_0}) \cdot \vec{n} + const \tag{9}$$

To this distance, a constant distance is added, which is the same for all DU's. The χ^2 has to be in units of meters to be interpreted correctly. Thats why the time of arrivals have to be converted into lengths by multiplying them with c. Then they can be compared with the calculated distance in the χ^2 function.

$$\chi^2(\theta, \phi, t_0) = \sum_i \left(\frac{t_i^{\text{meas}} \cdot c - (t_0 \cdot c + (\vec{x_i} - \vec{x_0}) \cdot \vec{n}(\theta, \phi)}{\sigma_i} \right)^2 \tag{10}$$

With the constant offset $t_0 \cdot c$ and the errors σ_i which are assumed to be all the same. By minimizing this function, `Iminuit` can find values for the parameters of interest θ, ϕ and the time offset t_0.
The position of the ship at the surface can be reconstructed by assuming the z position of this point as 0 and starting at x_0, adding the unit vector until reaching the surface

$$0 = x_0^z + \lambda \cdot n^z \longrightarrow \lambda = -\frac{x_0^z}{n^z} \tag{11}$$

$$x_{ship} = x_0 + \lambda \cdot \vec{n} \tag{12}$$

The position of the ship at surface is a nice way of displaying the results because the angles are much harder to interpret and compare.

7.2 Results of the Fit

Before the data could be fitted, some challenges needed to be solved. The actual ship position was not clear, so a grid search of the χ^2 function had to be performed to get better initial guesses for the fit parameters. With the initial guesses, the fit was able to reconstruct the direction of the incoming signal very well as displayed in figure 14. The direction vector points in the right direction, so the shape of the trajectory is correct. However, the whole trajectory appears to be shifted in space. This shift happens because all detection units (DU's) were projected onto one single center point $\vec{x_0}$ in the fit. The direction is then fitted based on this point, which

makes the reconstruction simpler, but also causes an offset. The direction stays the same, but the position is slightly shifted. For this fit, data from six of the DU's was used. To ensure, that `Iminuit` finds the correct solution, limits were applied to the polar angle so that the mirror solution is ruled out.

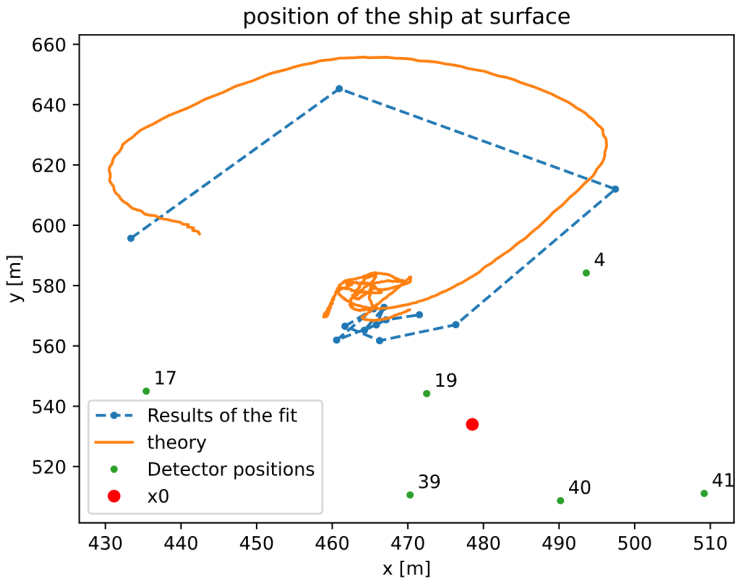

Figure 14: True trajectory and reconstructed trajectory. The direction is correct, but the trajectory is shifted because the DUs were projected to one center point $\vec{x}_0$.

This is not a central problem for this fit, where only the rough direction is the goal, but if the full trajectory in space is needed, a more complex model that includes the real positions of the DU's should be used. Despite the offset, the fit gives a very useful estimate of the direction of the signal. In many applications, such as determining where the signal came from in the sky or linking the signal to an astrophysical source, this direction is the most important result. The method is also fast and reliable, which makes it practical to apply for a first test on the recovered data.

8 Spherical Fit (Multilateration)

The goal of this fit is to reconstruct a precise position of the ship. This can be done by using the distance from each DU to the ship. This distance can be interpreted as the radius of a sphere around the DU. Each DU will have a sphere with a different radius as it has a different distance to the ship. The position of the ship is defined as the intersection point of all the spheres. In three dimensions, three points are needed to recreate a position. This process shown in figure 15 is called trilateration.

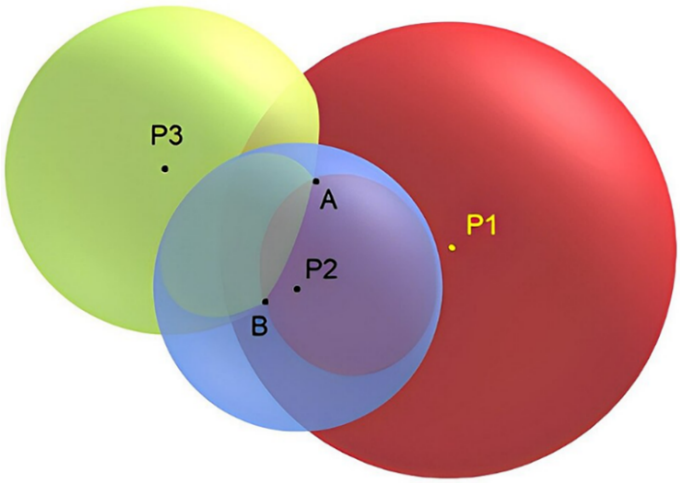

Figure 15: A nice illustration of the sphere problem. The intersection points A and B are mirror solutions [18].

In three dimensions, there is either a precise solution or no solution for the intersection point of three spheres but if you add more like in this case, there will not be a clear intersection point, but only an approximation. By adding more anchor points the problem changes from trilateration to multilateration. Like in the other problem, there are mirror solutions but only one is physically correct. The other one would be under the sea floor, and it can be again avoided by applying limits to the parameters.

8.1 Model

In the spherical model, it is assumed that a signal is emitted from an unknown point source at position $\vec{x}_{ship} = (x_s, y_s, z_s)$. The signal propagates at first approximation isotopically through the medium with a constant speed c, forming a spherical wavefront. The DU's are located at fixed positions $\vec{x}_i$ and the record time is given by $t_i^{\text{theo}} = \frac{1}{c} \cdot (\vec{x}_i - \vec{x}_{ship})$. The next step would be to model the speed of sound dependent on the depth. This of course means that there are no perfect spheres anymore, but the idea of the fit stays the same. In a realistic underwater environment such as the Mediterranean Sea at the ORCA site, the speed of sound is not constant, but depends on the depth. This depth dependence must be included in the model in order to get better results. But no matter how the modeled times t_i^{theo} are calculated, the χ^2 function has the same form:

$$\chi^2(x_s, y_s, z_s, t^{\text{emit}}) = \sum_i \left(\frac{(t_i^{\text{meas}} - (t_i^{\text{theo}} + t^{\text{emit}})) \cdot c}{\sigma_i} \right)^2 \tag{13}$$

where σ_i denotes the uncertainty in the measurement and is assumed to be the same for all detectors. The minimization is performed with respect to the spatial

coordinates of the source (x_s, y_s, z_s) and the time offset t^{emit} which is important because the time of arrival (ToA) values are not calibrated to the time of emission so it has to be part of the fit.
A simple way of implementing a variable sound speed $c(z)$ is by assuming a path from the emitter to the receiver. The speed of sound along this path is dependent on the position on the path. Assuming a sound wave travels along a straight-line path in three-dimensional space, the travel distance depends on the local speed of sound, which may vary with a dependency on the depth z. Let the unit vector of the direction of the wave be denoted by $\hat{n}$, and let the path be parameterized by a scalar λ such that

$$\vec{r}(\lambda) = \vec{r}_0 + \lambda\hat{n} \tag{14}$$

where $\vec{r}_0$ is a reference point on the path (e.g. the emission point).

If the sound speed depends on the vertical position (depth), i.e. $c = c(z)$, then the local speed along the path becomes $c(\vec{r}(\lambda)) = c(z(\lambda))$. Since the differential path length is $\mathrm{d}l = |\mathrm{d}\vec{r}| = |\hat{n}|\,\mathrm{d}\lambda = \mathrm{d}\lambda$, the total travel time t from $\lambda = 0$ to $\lambda = L$ is given by

$$t = \int_0^L \frac{\mathrm{d}\lambda}{c(z(\lambda))} \tag{15}$$

This integral accounts for the fact that the sound wave travels at different speeds depending on the depth $z(\lambda)$ along its path.

$$t_i^{\text{model}} = \int_{\vec{r}_s}^{\vec{r}_i} \frac{1}{c(z)}\,\mathrm{d}\ell \tag{16}$$

Different models for the speed of sound can be plugged into this formula by changing $c(z)$ appropriately [19]. For this fit, different models for the speed were tested. The first step, changing from a constant speed of sound to a better approximation is a linear model as demonstrated in figure 16. This describes how the sound speed changes very accurately after a certain depth, but at the top it fails. In ORCA, the use of this model is valid, because all the trilateration is done under water near the sea floor.

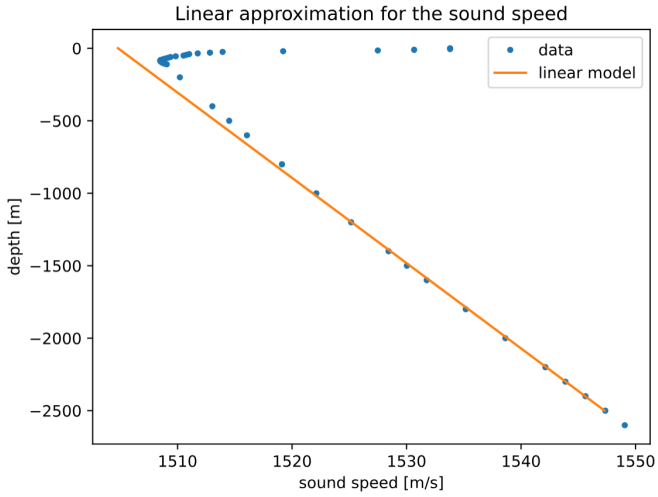

Figure 16: The model for the linear speed of sound used in the calculations and widely used in Km3NeT for underwater triangulation where the deviation at the surface is irrelevant.

This approximation is in general better in describing the time of flight in these situations as the model of a constant sound speed but it is still not accurate at the surface. For this fit, the behavior of the surface is relevant that's why the speed of sound is modeled different for this purpose. By interpolating the data measured, an almost perfect function of the sound speed can be acquired as shown in figure 17. When or if this is useful at all will be discussed in the results. Cubic interpolation was chosen in this case. This new sound speed profile can be again plugged in the path integral formula to get the time from point one to point two.

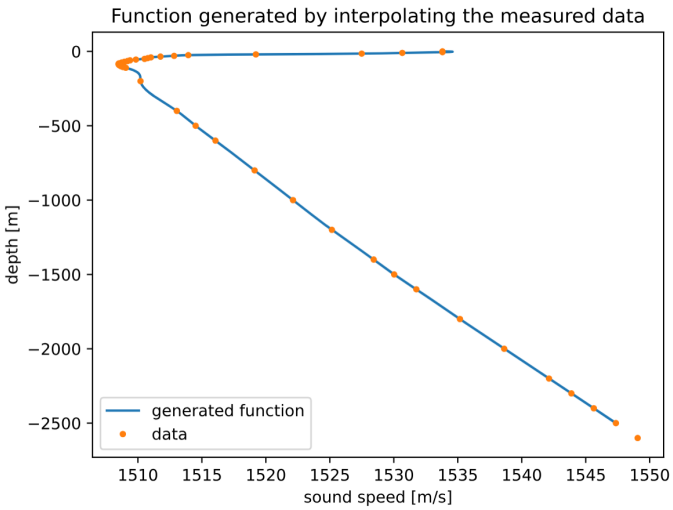

Figure 17: This model describes the behavior of the speed of sound more accurate and can possibly be used to reduce the errors of the fit.

8.2 Results of the Fit

The results of this fit need to be analyzed carefully in order to obtain the correct errors in the x an y position. The model still has systematic errors. These errors are not represented in the outputs of `Iminuit`. The first way to analyze the results is to again plot the coordinates of x and y of the GPS positions and the reconstructed positions. Figure 18 shows the results for the linear model of the sound speed. This looks almost the same for both the linear and the interpolated model, so only the result of one is displayed this way.

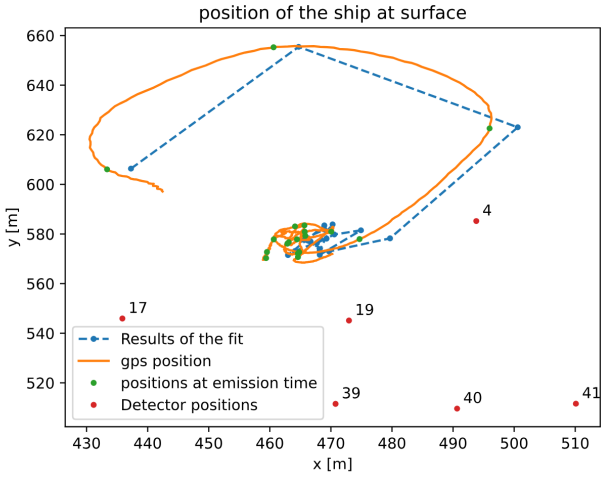

Figure 18: In contrast to the fit of direction the position got reconstructed almost perfectly but there is a constant offset visible which is caused by systematic errors.

Systematic errors in the fit come from the fact that the model used is not fully accurate. The biggest sources of error are the model of the speed of sound and the assumption that the sound travels in a straight line. In reality, the speed of sound changes with depth, and this causes the signal path to bend, which is not taken into account in a simple spherical model. This means the calculated distances based on arrival times can be slightly wrong. Other disturbances like small time offsets or signal reflections can also affect the result and lead to a small additional offset in the reconstructed position. Two models for the speed of sound were tested. To see, which one is more accurate the systematic errors for both cases can be determined and compared like in figure 19. To estimate the systematic errors, the distance between the GPS and the reconstructed position can be plotted in a histogram. A gaussian fit of this histogram data gives the mean value μ which can be interpreted as the systematic error and the standard deviation σ which would be a rough estimate of the overall error [20].

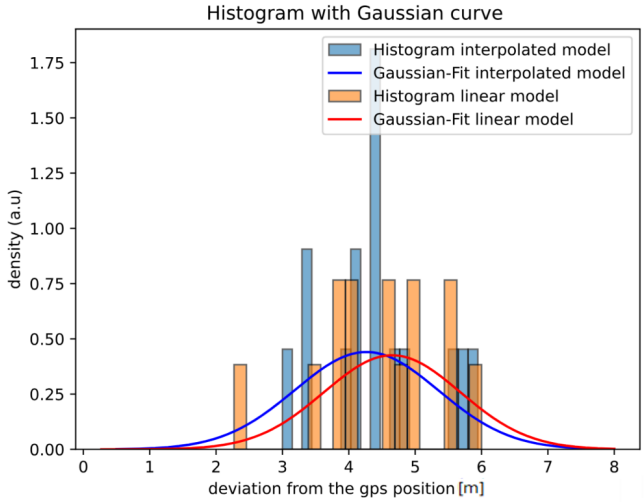

Figure 19: Results of the fit: $\mu_1 = 4.2 \pm 0.5$ $\sigma_1 = 1.1 \pm 0.4$ and $\mu_2 = 4.7 \pm 0.4$ $\sigma_2 = 1.1 \pm 0.8$. It can be seen that the interpolated data is shifted to the left which means it is slightly closer to the gps position than the linear model.

Due to the smaller μ_1, it can be concluded that the systematic error is slightly reduced by implementing the more detailed model of the sound speed. The Parameter σ consists of combined uncertainties, including statistical and model errors. To obtain the x and y errors the outputs of `Iminuit` can be taken. For consistency reasons the σ values of the gaussian fit should be round about the same as the Hesse errors of `Iminuit` and it turns out they are. Some parameters of the fit had limits applied to ensure that the correct solution is found but the limits are counterproductive for error analysis due to the trigonometric projection. That's why the fit has to be redone with the exact positions that came out earlier as the starting values. By doing this, the following errors for different signals are obtained:

Index	1	2	3	4	5	6	7	8	9	10	11	12	13
σ_x [m]	1.2050	1.2069	1.2062	1.2046	1.2043	1.2035	1.4774	1.2031	1.0961	1.2050	1.2052	1.4763	1.4751
σ_y [m]	1.0335	1.0315	1.0237	1.0213	1.0320	1.0297	1.0993	1.0331	1.1124	1.0318	1.0332	1.1668	1.0975

Table 1: Uncertainties of x and y positions from the fit. The mean values $\pm$ standard deviations are: $\bar{\sigma}_x = 1.2\,\mathrm{m} \pm 0.1\,\mathrm{m}$ and $\bar{\sigma}_y = 1.05\,\mathrm{m} \pm 0.04\,\mathrm{m}$

These values give an idea of how precisely the position of the ship can be reconstructed using the hydrophones. The slightly smaller error in the y-direction could be due to the geometry of the detector setup. Although the detection units (DU's) are a little more spread along the x-axis, this actually improves the accuracy of the y-position. Since the hydrophones cover a wider range in x, the arrival times of the signals are more sensitive to changes in the y-direction. This means that the fit can better constrain the y-coordinate of the ship. In contrast, variations in x are a little harder to detect because the DUs are not distributed across y to the same extent. As a result, the mean error in y is slightly smaller than in x. All in all, the the

results hint, that the systematic error of the fit can be reduced by implementing the non linear depth dependency of the speed of sound but the deviation to the GPS position still is about four to five meters. The internal error caused by uncertainties in the measurements, disturbances of the signal in the water or most importantly correlations of the fit parameters, accumulates to an uncertainty a little over one meter in the x and y direction. The errors could be reduced by adding more degrees of freedom to the system which means in this case using more detection units.

9 DU positioning via Multilateration

Locating the positions of the DU is the actual goal of the whole procedure. Normally the position is determined via triangulation with the help of the acoustic beacons placed in a short distance around the DU's. It is very important to have data from different sides because the triangulation method relies on the intersection of spheres discussed earlier. If these spheres are not placed around the target, then there might be no overlap of the spheres due to errors. In this case the positions and emission times of the ship are known and utilizing them and the time of arrivals the position of the DU's can be reconstructed. With the data received from the ship the concept from before still holds so it's important to take many different ship positions that are spaced around the detector in order to make this work.

9.1 Model

To reconstruct the positions of the DUs, the time of emission and the time of arrival (ToA) of each signal are used together with the position of the ship at the time of emission. The ship's position is not directly measured for each signal but reconstructed by interpolating the GPS data. This interpolation gives an estimate of the ship's position at the moment when each signal was sent.

The main idea of the model is that the sound propagates spherically from the ship, and reaches each hydrophone after a time delay that depends on the distance and the speed of sound. By taking the time of emission and the corresponding ToA, the distance the signal has travelled can be calculated as

$$r_i = c \cdot \int_{\vec{r}_s}^{\vec{r}_i} \frac{1}{c(z)} \, \mathrm{d}\ell \tag{17}$$

the time calculated via a path integral scaled with the constant c. For this model, the interpolated function gathered from measurement data is used to get the best results.

A χ^2-function is constructed to quantify the agreement between the expected dis-

tances from the ship to the DU and the distances derived from the times. Additionally, a time offset dt is implemented because ORCA was not perfectly synchronized with the GPS of the ship.

$$\chi^2 = \sum_i \left(\|\vec{x}_{\text{DU}} - \vec{x}_{\text{ship},i}\| - r_i - dt \cdot c \right)^2 \tag{18}$$

The minimization of this χ^2-function gives the best estimate for the DU position that fits all measurements. The fit is performed using the `Iminuit` package. This method uses the timing and position information of the ship for as many signals as possible to reconstruct the hydrophone positions with high precision.

9.2 Results of the Fit

The accuracy of the reconstruction of the DU's positions is directly dependent on the accuracy of the data used. The fit was tested for all DU's, even the ones that had a time offset in the ToA data. DU9 is not included because its data for the second run was not recovered. As a start, the result of the fit for every DU is plotted at once in figure 20 to give an overview. The errors can then be analyzed separately.

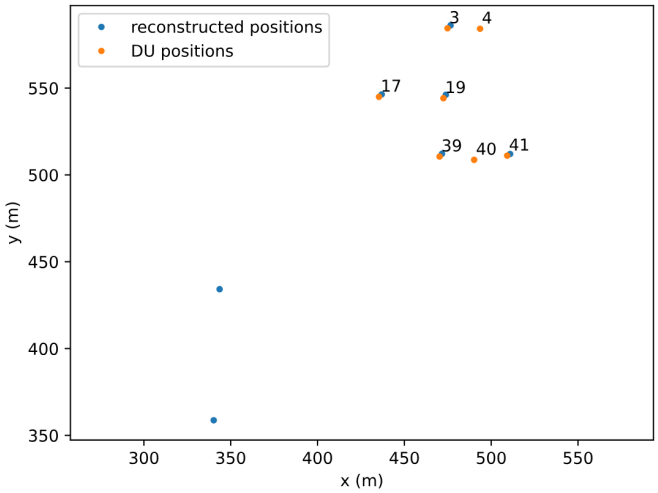

Figure 20: The position of most DU's at the sea floor got reconstructed almost perfectly but there where positioning offsets with number 4 and 40.

It was expected, that the positioning of DU4 could fail, it was even filtered out earlier because its data for the second run was faulty. Exactly what happened with nr. 40 is not clear. The data of the other ones is good and their results can be analyzed. The errors in the fitted DU positions mainly originate from two things. First, there can be small delays or noise in the timing of the ToA measurements for example, due to hardware jitter, the electronic timing resolution, or the way the signal crosses the threshold to be detected. So even if the signal is clean, the

exact arrival time might still be a bit off. Second, the ship positions used in the fit result from GPS data that had to be interpolated to get the estimated position at the exact time of emission. The positions of the ship are saved every second so if the GPS points are not very dense or the ship moves irregularly, the linear interpolation might not give the exact correct position at the time of emission. To get an estimation of the systematic error, the mean value and the standard deviation of the distances to the real positions can be observed: $\mu = 1.2$, $\sigma = 0.2$. The reason why the errors are much smaller in this fit compared to the previous ones is likely due to a few combined factors. First of all, the emission time was taken from the data and not part of the fit, which gives it fewer variables to optimize and makes the result more stable. Another big difference is the number of degrees of freedom: this fit used 23 signals to determine one position, which gives the fit a lot more data to rely on. That also means that small measurement errors like ToA uncertainties or timing jitter from the hardware do not have such a strong effect anymore, because they can average out across many signals.

The fit was started with all parameters open. Due to a very strong correlation between the time offset dt and the z coordinate, this led to problems with the correlation matrix. The positions of the ship were approximately directly over the detector so a shift in time is equal to a shift in z so they were nearly 100% correlated. So, the value of dt is fixed in the next step. This value was 0.24 s and it accounts not only for the wrong synchronization but also for a simplistic speed of sound model or other systematic errors. After fixing dt to this value, the fit stabilized.

For a correct error analysis the limits of the parameters were lifted and the errors had to be rescaled so that the value of the χ^2 function equals the degrees of freedom [17] [14]. With dt fixed, the fit parameters were the coordinates of the DU's so with 23 signals and ship positions used, the number of degrees of freedom is 20. Figures 21 , 22 and 23 show how the outputs of the fit for DU17 are displayed as an example.

Migrad

FCN = 20.08	Nfcn = 121
EDM = 0.000182 (Goal: 0.0002)	
Valid Minimum	Below EDM threshold (goal x 10)
No parameters at limit	Below call limit
Hesse ok	Covariance accurate

Figure 21: The final minimum is normalized to the degrees of freedom and the number of tries as well as the distance to the minimum are displayed. All in all its a valid minimum and there are no warnings.

	Name	Value	Hesse Error	Minos Error-	Minos Error+	Limit-	Limit+	Fixed
0	x	435.76	0.23					
1	y	546.23	0.16					
2	z	-2.449160e3	0.000014e3					
3	dt	0.2400	0.0024					yes

Figure 22: The values of the fit parameters are displayed along with their Hesse errors. No limits are applied and *dt* is fixed.

	x	y	z	dt
x	0.0508	-0.023 **(-0.622)**	-1.34e-3 **(-0.415)**	0.00
y	-0.023 **(-0.622)**	0.0265	-0.39e-3 **(-0.167)**	0.000
z	-1.34e-3 **(-0.415)**	-0.39e-3 **(-0.167)**	0.000205	0
dt	0.00	0.000	0	0

Figure 23: The correlation matrix of DU 17

The strongest correlation is observed between the x and y coordinates, with a correlation coefficient of -0.622. This moderately strong negative correlation implies that variations in x are compensated by opposite variations in y during the fit. A moderate negative correlation is also found between x and z (-0.415), while the correlation between y and z is weaker (-0.167). These values indicate some degree of parameter coupling but are not considered critical. The error in x and y is in general much higher than the error in z this is also seen in the correlation matrix because they are correlated stronger. This means that a change in x can be easily compensated in a small change in y this often leads to a less steep χ^2 function at the minimum which is what the errors are defined by. An explanation for these bigger errors might be the interpolated x and y coordinates of the ship while the z coordinate was held constant at $-2.7\,\mathrm{m}$ because that is the position of the emitter on the ship. In Table2, the Hesse errors for all DU's are summarized.

Table 2: Position uncertainties from the fits in x, y, and z directions (in meters).

DU	σ_x **[m]**	σ_y **[m]**	σ_z **[m]**
39	0.217	0.209	0.015
40	-	-	-
41	0.226	0.149	0.013
4	-	-	-
19	0.126	0.116	0.012
17	0.225	0.163	0.014
3	0.049	0.087	0.012

The errors are fairly consistent but for DU3, the x and y errors are smaller than for the other detection units. The correlation matrix for DU3, which is shown in

figure 24, is also different from the others. The correlations for x and y are much smaller in this case.

	x	y	z	dt
x	0.00243	0.0020 **(0.468)**	-0.18e-3 **(-0.322)**	0.0000
y	0.0020 **(0.468)**	0.00762	-0.43e-3 **(-0.419)**	0.000
z	-0.18e-3 **(-0.322)**	-0.43e-3 **(-0.419)**	0.000135	0
dt	0.0000	0.000	0	0

Figure 24: The correlation Matrix of DU3 differs from the others in the correlations of x and y.

The reason why the errors of DU3 are smaller could lie in the track of the ship which is displayed in figure 25. During the first run, the ship had a phase where it stopped directly over DU3 and hardly moved. Although the same signal data were used to fit the positions of all DUs, DU3 ends up with much smaller uncertainties.

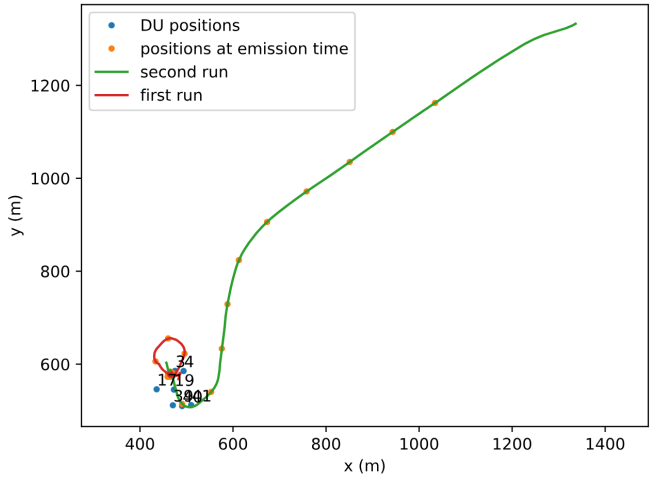

Figure 25: A cluster of 10 data points is located exactly over DU3 this leads to smaller errors.

Because of this, the signal arrival times at DU3 are especially useful for narrowing down its exact position. Small uncertainties in the emission time or the ship's position don't affect the result as much for DU3 as they do for DUs that are further away. The fit can "lock in" the position of DU3 more precisely. This geometric advantage can lead to smaller errors in the final result for DU3, even though all DUs had the same signal input.

Overall, it was a successful reconstruction of detection unit (DU) positions using the arrival times of acoustic signals and interpolated GPS positions of the emission source. Despite minor issues with some units, the majority of the fits produced

highly accurate results, with position uncertainties way under a meter. The analysis demonstrated that signal geometry, especially the spatial distribution of emission points, plays a crucial role in the precision of the reconstruction, as seen with DU3. The systematic offset in emission time could be effectively accounted for by introducing dt, and the overall behavior of the χ^2 function confirmed the validity of the fits.

10 Summary and Conclusion

In this work, the positions of acoustic signal sources and detection units (DU's) in the KM3NeT-ORCA detector were reconstructed using arrival times of sound waves and the method of multilateration. The direction of the signal was first estimated using a simplified plane wave model, which worked well for getting the angles but introduced a spatial offset because the DUs were projected to a central point and the model used a most simplified speed of sound, which assumed a constant speed which in reality, is not accurate. To improve accuracy, a spherical model was used that considers real positions of all DUs and includes different models for the depth-dependent speed of sound. It turned out that the speed of sound model has a noticeable effect on the result. The interpolated sound speed profile reduced the systematic offset between reconstructed and GPS positions by about 0.5 m compared to a simple linear model. Still, there remained a systematic deviation of around 4 m, likely caused by remaining model assumptions like straight-line propagation. The internal errors due to uncertainties in arrival time and parameter correlations were about 1.2 m in x and 1.05 m in y direction. These were consistent with the error estimates from the Gauß-fit. Finally, the same method was successfully used in reverse to reconstruct DU positions based on known ship locations. The average error was below 0.2 m for most DUs, showing that the method is reliable when sufficient high-quality data is available. It was shown that more signal paths and better spatial distribution of sources lead to smaller uncertainties. The geometry of the problem had also an effect on the errors as observed with DU3. Overall, the results show that this alternative acoustic positioning in KM3NeT can work with sub-meter-level precision, but model improvements and careful calibrations are crucial for reducing both statistical and systematic errors.

I would like to thank Sharif El Mentawi and Vincent Bertin (CPPM) for providing the processed data used in this analysis, and for always being available for questions and discussions.

References

[1] Julia K. Becker. *High-Energy Neutrino Astrophysics*. Vol. 875. Lecture Notes in Physics. Springer, 2013. ISBN: 9783642394712.

[2] Wikipedia contributors. *KM3NeT — Wikipedia, The Free Encyclopedia*. https://en.wikipedia.org/wiki/KM3NeT. Accessed July 13, 2025. 2024.

[3] S. Adrián-Martínez et al. "Letter of intent for KM3NeT 2.0". In: *Journal of Physics G: Nuclear and Particle Physics* 43.8 (2016), p. 084001. DOI: 10.1088/0954-3899/43/8/084001.

[4] KM3NeT collaboration. *Logbook entry on the 9th of July Mission*. Accessed: 2025-06-14. 2024. URL: https://elog.km3net.de/Operations+FR/11059.

[5] KM3NeT collaboration. *KM3NeT opens a new window in our universe*. Accessed: 2025-06-14. 2025. URL: https://www.km3net.org/.

[6] Robert J. Urick. *Principles of Underwater Sound*. 3rd. McGraw-Hill, 1983. ISBN: 9780070660870.

[7] Kevin D. Heaney et al. "Ocean acoustic propagation models". In: *IEEE Journal of Oceanic Engineering* 39.4 (2014), pp. 782–802. DOI: 10.1109/JOE.2014.2321572.

[8] S. Adrián-Martínez et al. "KM3NeT 2.0—Technical Design Report". In: *arXiv preprint arXiv:1601.07459* (2016). URL: https://arxiv.org/abs/1601.07459.

[9] S. Aiello et al. "Measurement of the atmospheric muon flux with the first KM3NeT detection units". In: *The European Physical Journal C* 82.3 (2022), pp. 1–19. DOI: 10.1140/epjc/s10052-022-10144-3.

[10] J. A. Aguilar et al. "The data acquisition system of the KM3NeT detector". In: *Sensors* 20.17 (2020), p. 4826. DOI: 10.3390/s20174826.

[11] P. Piattelli et al. "KM3NeT positioning system: performances and first results". In: *EPJ Web of Conferences* 207 (2019), p. 02006. DOI: 10.1051/epjconf/201920702006.

[12] A. D. Pierce. *Acoustics: An Introduction to Its Physical Principles and Applications*. McGraw-Hill, 1989.

[13] C. T. Chen and F. J. Millero. "Speed of sound in seawater at high pressures". In: *The Journal of the Acoustical Society of America* 62.5 (1977), pp. 1129–1135.

[14] Fred James and Michel Goossens. *MINUIT: Function Minimization and Error Analysis Reference Manual*. CERN Program Library Long Writeup D506. CERN. Geneva, 1998.

[15] Hans Dembinski et al. *iminuit – A Python interface to MINUIT*. Accessed: 2025-06-14. Scikit-HEP. 2024. URL: `https://iminuit.readthedocs.io/`.

[16] Larry Wasserman. *All of Statistics: A Concise Course in Statistical Inference*. Springer, 2004. ISBN: 9780387402727.

[17] Philip R. Bevington and D. Keith Robinson. *Data Reduction and Error Analysis for the Physical Sciences*. 3rd. McGraw-Hill, 2003. ISBN: 9780072472273.

[18] Tomasz Ludyga. "Entwicklung und Untersuchung eines Konzepts zur Nutzung von Indoor-Positioning-Technologie in Systemen für adaptive, mobile Informationsbereitstellung". Bachelor's Thesis. Technische Universität Dresten, 2018.

[19] George B. Arfken, Hans J. Weber, and Frank E. Harris. *Mathematical Methods for Physicists*. 7th. Academic Press, 2012. ISBN: 9780123846549.

[20] UNC Physics Department. *Measurement and Uncertainty Analysis Guide*. `https://users.physics.unc.edu/~deardorf/uncertainty/UNCguide.pdf`. Accessed: 2025-06-14. 2015.

A Measurement data

Table 3: Speed of sound profile

Depth [m]	Velocity [m/s]
0.000	1533.803
5.006	1533.803
10.005	1530.662
15.006	1527.491
20.008	1519.221
25.008	1513.936
30.001	1512.830
35.008	1511.763
40.025	1511.013
45.016	1510.768
50.010	1510.523
55.001	1509.843
60.001	1509.382
65.027	1509.176
70.015	1508.938
75.005	1508.725
80.007	1508.517
85.014	1508.479
90.006	1508.514
95.001	1508.584
100.017	1508.691
105.010	1508.835
110.007	1509.053
200.0	1510.203
400.0	1513.040
500.0	1514.510
600.0	1516.060
800.0	1519.120
1000.0	1522.120
1200.0	1525.160
1400.0	1528.430
1500.0	1530.030
1600.0	1531.760
1800.0	1535.170
2000.0	1538.630
2200.0	1542.130
2300.0	1543.880
2400.0	1545.630
2500.0	1547.360
2600.0	1549.060